Physicochemical Investigations on Solid Lipid Nanoparticles and on Oil-Loaded Solid Lipid Nanoparticles: A Nuclear Magnetic Resonance and Electron Spin Resonance Study

Katja Jores,[1] Wolfgang Mehnert,[1] and Karsten Mäder[2,3]

Received January 28, 2003; accepted April 30, 2003

Purpose. Recently, colloidal dispersions made of mixtures from solid and liquid lipids have been described to combine controlled-release characteristics with higher drug-loading capacities than solid lipid nanoparticles (SLNs). It has been proposed that these nanostructured lipid carriers (NLCs) are composed of oily droplets that are embedded in a solid lipid matrix. The present work investigates the structure and performance of NLCs.

Methods. Colloidal lipid dispersions were produced by high-pressure homogenization and characterized by laser diffraction, photon correlation spectroscopy, wide-angle x-ray scattering, and differential scanning calorimetry. Proton nuclear magnetic resonance spectroscopy and electron spin resonance experiments were performed to investigate the mobility of the components and the molecular environment of model drugs. Furthermore, a nitroxide reduction assay with ascorbic acid was conducted to explore the accessibility of the lipid model drug from the outer aqueous phase.

Results. Proton nuclear magnetic resonance spectra clearly demonstrate that NLC nanoparticles differ from nanoemulsions and from SLNs by forming a liquid compartment that is in strong interaction to the solid lipid. The electron spin resonance model drug was found to be accommodated either on the particle surface with close water contact (SLN) or additionally in the oil (NLC). The oil compartment must be localized on the particle surface, because it can be easily reached by ascorbic acid.

Conclusion. Neither SLN nor NLC lipid nanoparticles showed any advantage with respect to incorporation rate or retarded accessibility to the drug compared with conventional nanoemulsions. The experimental data let us conclude that NLCs are not spherical solid lipid particles with embedded liquid droplets, but they are rather solid platelets with oil present between the solid platelet and the surfactant layer.

KEY WORDS: solid lipid nanoparticles; colloidal carrier; nanoemulsion; ESR; NMR; SLN; NLC.

INTRODUCTION

Colloidal drug carriers offer a number of potential advantages as delivery systems, such as better bioavailability for poorly water-soluble drugs. Beside nanoemulsions, nanosuspensions, mixed micelles, and liposomes, melt-emulsified nanoparticles based on at room temperature solid lipids have been developed (1). The advantages of solid lipid nanoparticles (SLNs) are the use of physiological lipids, the avoidance of organic solvents, a potential wide application spectrum (dermal, per os, intravenous), and the high-pressure homogenization as an established production method, which allows large-scale production. Additionally, improved bioavailability, protection of sensitive drug molecules from the outer environment (water, light), and even controlled-release characteristics have been claimed (2,3).

Common disadvantages of SLNs include particle growing, unpredictable gelation tendency, unexpected dynamics of polymorphic transitions, and inherent low incorporation rates resulting from the crystalline structure of the solid lipid (4–6). It has been proposed that this last mentioned drawback can be overcome by oil-loaded solid nanolipids (also described as nanostructured lipid carriers, or NLCs; Refs 7 and 8). Liquid lipids solubilize the drug to a much higher extent than solid lipids. In a preferred scenario, the liquid lipids form inner droplets in the solid nanoparticles. In this model, the NLC nanoparticles would provide a high incorporation rate (because of the liquid lipid) and a controlled release (because of the outer solid lipid). It has been postulated that medium-chain triglyceride (MCT) molecules can replace glyceryl behenate (GB) molecules in the crystal lattice in a random distribution up to a MCT load of 16% (weight % of total lipid; Refs 7 and 9). Even higher oil loads up to 38% (weight % of total lipid) have been described to be incorporated as MCT clusters inside the solid matrix. It was the aim of the present study to get experimental evidence on the postulated structures and to investigate the physicochemical characteristics of the NLC in more detail.

Particle size was measured by laser diffraction (LD) and photon correlation spectroscopy (PCS). Differential scanning calorimetry (DSC) and x-ray measurements were used to judge the extent of crystallization and the polymorphic state of the lipids. Further results on the interaction of the oil with the solid lipid matrix were obtained by nuclear magnetic resonance spectroscopy of the protons (^{1}H-NMR). The mobility of the oil molecules is related to the width of the signal. Broad signals and weak amplitudes are characteristic for molecules of restricted mobility. Solid molecules are not detected by NMR under the experimental conditions due to very short relaxation times.

We also used electron spin resonance (ESR) to investigate the molecular environment (mobility, polarity) of the hydrophobic drug model compound tempolbenzoate (TB). In addition, the ability of the lipid phase to protect incorporated molecules from the aqueous environment was estimated by an ascorbic acid (AA) reduction assay. The assay is based on the reduction of the paramagnetic lipophilic nitroxide TB to the ESR silent hydroxylamine by the hydrophilic ascorbic acid. Rapid loss of the ESR signal intensity indicates high accessibility of the lipophilic model drug to the aqueous phase.

MATERIALS AND METHODS

Materials

Compritol 888 ATO (INCI: tribehenin, USP: glyceryl behenate, GB) is a mixture of approximately 15% mono-, 50%

[1] Institute of Pharmacy, Department of Pharmaceutical Technology, Free University of Berlin, Kelchstr. 31, 12169 Berlin, Germany.

[2] Institute of Pharmaceutical Technology and Biopharmacy, Martin-Luther-University Halle-Wittenberg, Wolfgang-Langenbeck-Str. 4, 06120 Halle/Saale, Germany.

[3] To whom correspondence should be addressed. (e-mail: Maeder@pharmazie.uni-halle.de)

0724-8741/03/0800-1274/0 © 2003 Plenum Publishing Corporation

di-, and 35% triglycerides of behenic acid (C_{22}), whereas other fatty acids than behenic acid account for less than 20%. The melting point lies between 69 and 74°C. It was a gift of Gattefossé (D-Weil am Rhein). Miglyol 812 (DAC: oleum neutrale; CTFA: caprylic/capric triglyceride (caprylic acid: C_8, capric acid: C_{10}), medium chain triglycerides; MCT) was provided by Caelo (D-Hilden). Lutrol F 68 (poloxamer 188; a polyoxyethylene-polyoxypropylene polymer) was donated by BASF (D-Ludwigshafen). Tempolbenzoate (4-Hydroxy-TEMPO benzoate, TB; melting point: 99–101°C) was obtained from Aldrich Chemicals (Milwaukee, WI, USA). Ascorbic acid (AA) sodium salt was ordered from Fluka (D-Steinheim). Deuterized water, chloroform-D1 and Uvasol™ (tetramethylsilane) were obtained from Merck (D-Darmstadt). Trimethylsilylpropionic acid sodium salt-2,2,3,3-D4 (TMS) from Deutero (D-Kastellaun) with its sharp signal at 0 ppm served as a NMR reference.

Methods

Preparation of SLN, NLC, and Nanoemulsions

To produce solid lipid nanoparticles GB was melted at 85°C in a water bath. In general, it is recommended to destroy any crystal center of the bulk material by a long heating phase clearly over the melting point with the aim to avoid the lipid memory effect and to make new crystallization possible (10). Various amounts of MCT in case of oil loading were added (2%, 4%, 10% w/w MCT, referred to the total lipid phase). The total lipid concentration amounts to 10% in the formulations. For ESR measurements 1 mmol TB was added. The hot lipid phase was given to an aqueous surfactant solution of 2.5% poloxamer 188 of the same temperature and a dispersion was formed using an ultra turrax (IKA, D-Staufen) for 30 s at 8000 rpm. The premix was passed through a Lab 40 high-pressure homogenizer (APV Gaulin, D-Lübeck). Three cycles at 85°C and 500 bar were performed. Controlled annealing of the dispersions happened in a water bath of 22°C in which the filled silanized glass vials were placed. Storage of the samples took place at 22°C, protected from light. The nanoemulsions were prepared in exactly the same manner replacing GB by MCT only. Mixed dispersions (MIX) were produced by mixing of separately produced solid (SLN) and liquid (NEmu) lipid nanodispersions.

An overview of all investigated formulations is given in Table I. All following measurements were performed or started, respectively, 1 day after sample production.

Particle Size Measurements

To estimate the average diameter and the polydispersity index of the anisometric lipid crystals, photon correlation spectroscopy (PCS; Zetasizer 4, Malvern Instruments, UK-Malvern) under an angle of 90° was used. Before measuring, each sample had to be diluted with demineralized particle-free water to an adequate intensity. Additionally, the laser diffraction method (LD) was used (Coulter LS 230; Miami, FL, USA). By its additional polarization intensity differential scattering (PIDS) technology this instrument is capable to measure particles down to 40 nm. For calculating the PIDS results refraction has to be estimated for the particles (1.456 as real refractive index and 0.01 as imaginary refractive index). Each dimensional information is expressed as median plus/minus range of three experiments, each performed in triplicate.

Nuclear Magnetic Resonance Spectroscopy Measurements

^{1}H-NMR spectra were recorded by an Avance DPX 400 spectrometer (Bruker, D-Rheinstätten), operating at 400 MHz and 20°C. An aliquot of each aqueous nanodispersion was filled in a NMR tube. Accurately weighted quantities of deuterized water (for all aqueous samples) or chloroform-D1 (for measurement of MCT/GB bulkware) were added for field login and TMS was added as reference for 0 ppm.

ESR Spectroscopy Measurements

An ESR equipment of 1.5 GHz (L-band) from Magnettech (D-Berlin) was used. The measurements were conducted at room temperature. The following typical parameters were used: modulation frequency, 100 kHz; microwave power, 50 mW; modulation amplitude, 0.01 mT; time constant, 0.06 s; scan time, 1 min; scan range, 10 mT. The reduction kinetics of the spin probe in the samples were gained by time depending ESR measurements after mixing (1:1 v/v) with 1.6 mM aqueous ascorbid acid salt solution. Further information on distribution of TB in the samples were obtained by adding spin probe to probe-free dispersions and following ESR measurements. Simulation of the ESR spectra was per-

Table I. Sample Compositions

Sample	% lipid (w/w)	% GB (w/w)	% MCT (w/w)	% poloxamer (w/w)	Production procedure
SLN	10	10	0	2.5	Homogenization of dispersions composed of mixtures of molten lipids
NLC-0.2	10	9.8	0.2	2.5	
NLC-0.4	10	9.6	0.4	2.5	
NLC-1.0	10	9	1	2.5	
NEmu-0.2%	0.2	0	0.2	2.5	
NEmu-0.4%	0.4	0	0.4	2.5	
NEmu-1%	1	0	1	2.5	
NEmu-10%	10	0	10	2.5	
Mix-0.2	10	9.8	0.2	2.5	Separate production of GB-SLN and MCT-nanoemulsion, followed by mixing of both dispersions in desired ratio
Mix-0.4	10	9.6	0.4	2.5	
Mix-1.0	10	9	1	2.5	

formed by means of the PEST-software from National Institutes of Health (Bethesda, MD, USA).

DSC Measurements

DSC was performed by a Mettler DSC 821 (Mettler Toledo, D-Gießen). In 40-μL aluminum pans accurately weighted dispersions (approximately 15 mg) were filled. Then, the pans were hermetically closed. DSC scans were recorded at a heating and cooling rate of 5 K/min, in comparison with an empty pan. It was made use of nitrogen as flush gas (80 ml/min). Melting points correspond to the maxima of the DSC curves.

X-Ray Measurements

Wide-angle x-ray scattering (WAXS; 2 Theta = 4–40°) was performed by a Philips x-ray generator PW 1830 (Philips, Amelo, The Netherlands), equipped with a copper anode (40 kV, 25 mA, wavelength 0.154178 nm) and a mobile counting tube (Goniometer PW 1820). Against loss of water, liquid samples were hold in the carrier by a Mylar film. Its own narrow diffraction signal could be eliminated mathematically by subtraction of a blank.

RESULTS

Particle Size Measurements

The particle sizes obtained by means of static (LD, PIDS included) and dynamic light scattering (PCS) methods are comparable (Table II). Nearly unaffected of the concentration of MCT (formulations SLN, NLC-0.2, NLC-0.4, NLC-1.0, NEmu-10%), nanoparticles of similar size range were obtained through both size measuring techniques. Slightly larger particles and an increase in the polydispersity index is seen for SLN and NLC with low oil loads. As the viscosity of MCT compared with GB at temperatures above 70°C was not found to differ (11), better homogenization efficiency owing to lower viscosity can be disregarded. However, nonspherical platelets as SLN are treated mathematically as spheres in LD. In PCS different particle shape causes different Brownian movement. Both methods depend highly on diluting the samples in water, which may result in tenside diffusion from the particle surface, however, particle sizes and polydispersity index can be considered as estimates only (12). Further inaccuracy is given through the used laser diffractometer. It combines the methods of diffraction and light scattering to one single result what is not recommended by the current regulatory (13).

The droplets of the nanoemulsion have by far the lowest polydispersity index and a slightly smaller particle size compared with GB-containing dispersions. Increasing MCT loads decreased the polydispersity index of the NLC particles, whereas the polydispersity index of the MIX samples was independent from the percentage of MCT. The particle sizes of samples made from physical mixtures of nanoemulsions and nanosuspensions are similar to the values of the nanosuspension.

Particle sizes of all samples remained unchanged during the measurement period of at least 4 weeks. They could be recovered even after the ESR reduction assay.

^{1}H-NMR Measurements

^{1}H-NMR spectra of the colloidal GB nanosuspension (formulation SLN) and the nanoemulsion made from MCT (formulation NEmu-10%) are shown in Fig. 1. In the SLN sample only poloxamer derived, but no GB-related signals are observed. This finding indicates that the nanoparticles have crystallized. The presence of supercooled melts, which have been observed by NMR for other "SLN"-samples (5, 12) can therefore be excluded.

To facilitate the assignment of the peaks to the ingredients in the complex colloidal mixtures, NMR spectra of aqueous poloxamer solution, poloxamer-free homogenized MCT-water mixtures, and GB–water mixtures were recorded (Fig. 2). Despite the absence of the poloxamer, both lipid dispersions showed a remarkable short-term stability (LD 99% <3 microns after 1 day), which permitted the NMR measurements. The absence of $-CH_2$ and $-CH_3$ NMR signals in GB–water mixture was expected because solid ingredients are not detected under the experimental conditions because of very short relaxation times. The ppm values of the MCT methyl and methylene protons ($-CH_3$: 0.9 and $-CH_2$: 1.3) are typical for alkyl chains of triglycerides. Protons located near or at the glycerol part of the lipid have higher ppm values. The ppm values for methyl and methylene groups of poloxamer can easily be distinguished from MCT signals, because they are shifted to higher values ($-CH_3$: 1.2 and $-CH_2$: 3.7) resulting from the presence of oxygen in the polymer backbone. The assignment of the NMR signals of MCT and poloxamer are in agreement with the literature (e.g., NMR databases and Reference 14).

The samples NEmu-0.2, NEmu-0.4, and NEmu-1.0 are

Table II. Particle Size Dependence of SLN on Different Oil Loads, Determined by Laser Diffraction (LD) and Photon Correlation Spectroscopy (PCS), Expressed as Median x (x_{min}; x_{max})

Formulation	LD: 50% (V) of all particles smaller than [nm]	LD: 99% (V) of all particles smaller than [nm]	PCS: average particle size [nm]	Polydispersity index (PCS)
SLN	205 (171; 227)	720 (669; 755)	250 (241; 268)	0.360 (0.339; 0.408)
NLC-0.2	199 (172; 267)	701 (679; 718)	266 (229; 286)	0.336 (0.275; 0.342)
NLC-0.4	199 (172; 237)	680 (645; 697)	259 (232; 279)	0.290 (0.211; 0.312)
NLC-1.0	196 (157; 270)	634 (623; 652)	266 (235; 274)	0.226 (0.210; 0.264)
NEmu-10%	161 (136; 198)	649 (595; 670)	182 (180; 193)	0.141 (0.111; 0.155)
Mix-0.2	197 (107; 247)	687 (567; 774)	246 (244; 267)	0.353 (0.329; 0.398)
Mix-0.4	184 (167; 241)	705 (655; 789)	242 (239; 260)	0.333 (0.313; 0.372
Mix-1.0	186 (167; 276)	719 (657; 749)	235 (225; 255)	0.328 (0.291; 0.420)

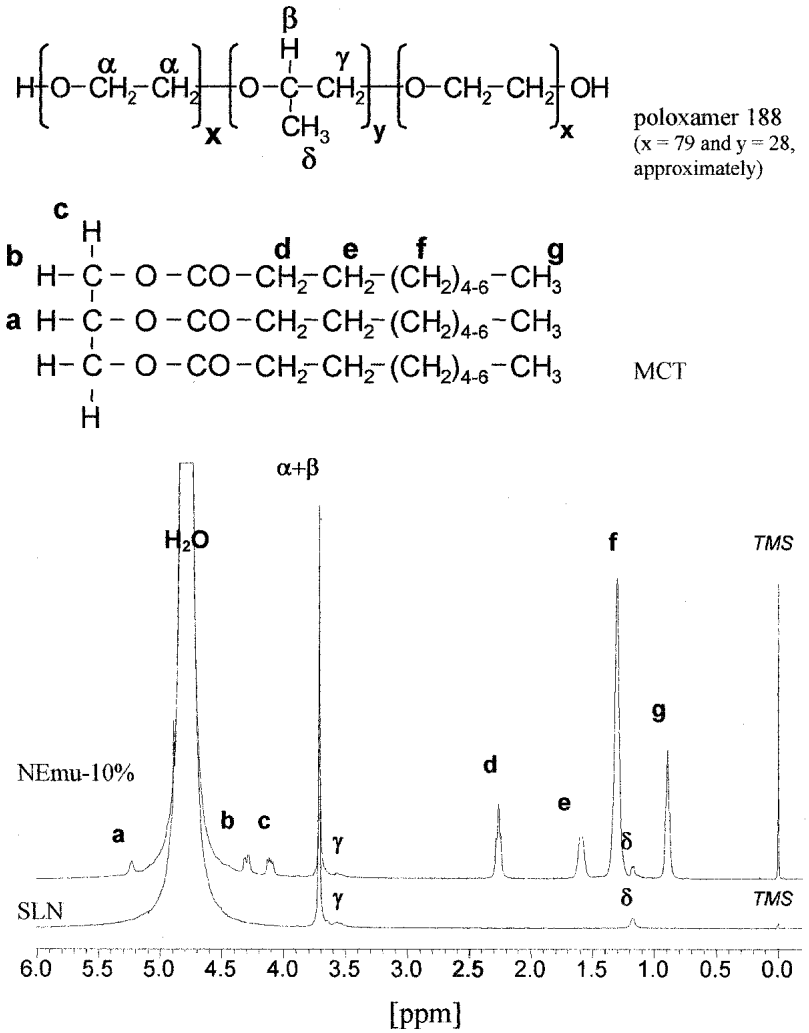

Fig. 1. Proton nuclear magnetic resonance spectra of the solid lipid nanoparticle formulation made from glyceryl behenate (bottom) and of the medium-chain triglycerides nanoemulsion (top). All signals are signed corresponding to the positions of the protons in the chemical formula above.

pure nanoemulsions with very low oil load (0.2, 0.4, and 1% w/w MCT and 2.5% poloxamer). NMR spectra were recorded without any sensitivity problem, which demonstrates that even such little oil amounts are detectable by means of NMR (spectra not shown). It was surprisingly found that the line widths of the MCT methylene protons in nanoemulsions are slightly smaller than those of MCT bulk because broader lines from restricted mobility of MCT molecules on the nanodroplet interface and line broadening caused by phase boundaries could be expected. Different viscosities could be one possible explanation. MCT formulated as nanodroplets experiences lower viscosity of the surrounding outer phase (viscosity of water: 1 mPa*s) whereas MCT bulk is more viscous (30 mPa*s). Moreover, for methylene protons of the bulk a very slightly more asymmetric signal was detected. Traces of water in the bulk could structure the oil and broaden the signal due to superpositions of different species. Additionally, phase boundaries with different magnetic susceptibilities might increase the NMR line width because of the introduction of local nonhomogeneities of the magnetic field.

The NMR spectra of NLC and MIX samples are quite different, although the chemical composition is the same and the sizes of the colloidal particles are comparable (Fig. 3). The MCT alkyl signals in NLC samples have much lower signal amplitudes due to broader lines, especially at lower oil loads. In contrast, alkyl signals of the MIX samples are comparable to pure nanoemulsions and the line width is equal for all MCT loads. The reason for increasing line widths and decreasing maximum amplitudes in the NLC samples is due to strong interaction of the oil molecules with solid GB what leads to an increased immobilization of the MCT molecules. Their relaxation is faster than that of unbound oil in the mixtures (15,16). Furthermore, the increase in line widths was more pronounced for the methyl end group of the lipid chain. The oil should be adhered on the solid lipid surface mainly by molecular affinities between lipophilic groups.

Previously described chemical shifts (9) of the fatty acids in GB–MCT systems can not be confirmed. The chemical environment of the oil molecules does not differ in particles with either high or low oil load. In this way, it can not be assumed that for low oil supplementation the oil molecules are surrounded by a matrix of solid GB, just as little higher oil

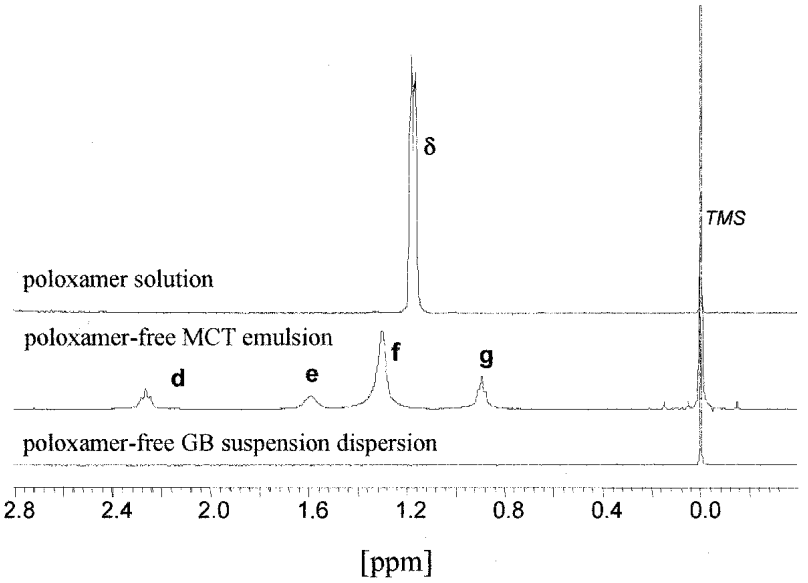

Fig. 2. Proton nuclear magnetic resonance spectra of a nonstabilized glyceryl behenate dispersion, of a nonstabilized medium-chain triglycerides emulsion and of an aqueous poloxamer solution (from the bottom to the top).

loads form clusters inside the particle. Most probable is the localization of the oil at the particle surface between solid glyceride and tenside layer (17,18). The extent of immobilization of the alkyl signals can be quantified by means of the widths at half height of the signal amplitude (Table III).

Attempts to quantify the immobilization of the MCT protons by adding the signal amplitude of the internal standard trimethylsilylpropionic acid sodium salt-D4 (TMS, signal at 0 ppm) failed because of the line broadening of TMS in solid lipid containing samples. We attribute this line broadening to adsorption and magnetization transfer processes similar to processes described by Mayer (19). The line broadening was considerable less pronounced in samples containing no solid lipid material. We attribute the higher increase in line width due to an increased surface area (platelet structure) and the higher rigidity of the interface.

The NMR line widths of the MCT protons in the MIX samples are in the range of the nanoemulsion. The NMR spectra of the mixed samples represent—in contrast to NLC—a superposition of the NMR spectra of SLN and NEmu. The small line widths of the MCT protons indicate no interaction of the liquid oil with the solid lipid. It can be concluded that steric stabilization stabilizes the particles very efficiently.

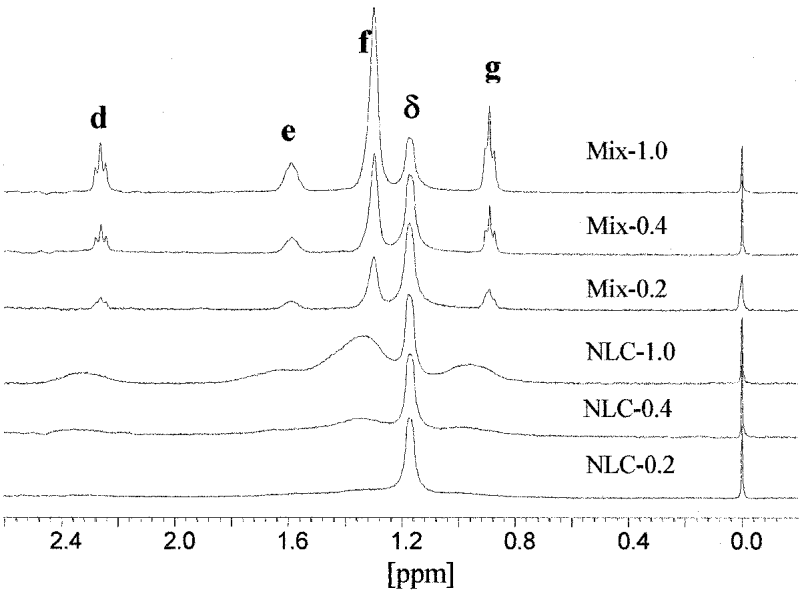

Fig. 3. Proton nuclear magnetic resonance spectra of hybrid lipid nanoparticles (formulations NLC-0.2, NLC-0.4, NLC-1.0) and mixtures from glyceryl behenate–solid lipid nanoparticles and medium-chain triglycerides nanoemulsions (Mix-0.2, Mix-0.4, Mix-1.0; from the bottom to the top).

Table III. Increased Widths at Half Height of Proton Nuclear Magnetic Resonance Signals as a Feature of Immobilized Chemical Groups

	Nuclear magnetic resonance line width at half amplitude [Hz]		
	Lipid–Protons		Poloxamer
Formulation	"f"-signal 1.3 ppm	"g"-signal 0.9 ppm	"δ"-signal 1.15 ppm
SLN	–	–	3.9
NLC-0.2	Approx. 96	Approx. 21	3.9
NLC-0.4	96.0	20.2	3.8
NLC-1.0	89.6	18.6	3.6
NEmu-10%	15.2	3.5	3.5
NEmu-0.2%	13.2	1.1	2.9
NEmu-0.4%	13.2	1.1	2.9
NEmu-1.0%	13.2	1.1	3.0
Mix-0.2	14.8	2.8	4.0
Mix-0.4	13.6	1.2	3.7
Mix-1.0	14.0	1.5	3.7
Glyceryl behenate dispersion without poloxamer	–	–	–
Medium-chain triglycerides dispersion without poloxamer	13.2	1.4	–
Oil bulk	20.8	3.4	–
Aqueous solution of poloxamer	–	–	2.9
Recrystall. melt of GB containing 2% oil (bulk-mixture)	signals unseparated: 296		–

The recrystallized melt of GB bulk containing 2% MCT is of great interest. A strong immobilization of MCT is given due to the rigid solid lipid matrix. In comparison even with the 2% oil loaded SLN, the bulk system let to broadened unseparated alkyl signals.

Concerning the tenside, slightly lower values for the widths at half height were obtained through increasing MCT load on the SLN. The reason can be found in different particle shapes: Higher oil content leads to more spherical particles and therefore less surfactant molecules are needed to stabilize the decreased surface area. During crystallization of the melt-emulsified glycerides poloxamer is able to stabilize the new areas efficiently enough to prevent particle agglomeration. In pure emulsions of absolutely low oil amounts the mobility of poloxamer is equal to an aqueous poloxamer solution. Furthermore, higher lipid content requires more tenside molecules which causes a higher level of immobilized molecules. In mixtures, the influence of the SLN on the widths at half height is predominant because of SLN's higher quantitative mixing ratios. Last of all, poloxamer seems to immobilize partly the alkyl groups of oil droplets what is shown in the comparison of a unstabilized nanoemulsion with its stabilized counterpart.

ESR Measurements

In the ESR spectra only paramagnetic (e.g., TB) but not diamagnetic substances as the used lipid or tenside provoke signals (20). TB (4-Hydroxy-2,2,6,6-tetramethylpiperidin-1-oxyl; Fig. 4a) belongs to the group of nitroxyl radicals. It is an at room temperature solid crystalline red substance of high lipophilicity (distribution coefficient n-octanol/water approx. 300). ESR permits the measurement of the molecular mobility (spectral shape) and the polarity of the molecular environment of the probe TB (hyperfine splitting constant a_N). The ESR spectra indicate that TB experiences different environments in nanoemulsions, SLN- and NLC-dispersions (Fig. 4b). Spectral simulation (Fig. 4c) permits a quantitative characterization (Fig. 4d) of the ESR spectra. The spectrum of the nanoemulsion can be simulated with a single species of high mobility in a lipophilic environment. This result agrees well with the expectation. Because of the high lipophilicity, the nitroxide will almost completely be dissolved in the oil. The ESR spectra of the SLN can be simulated by three different species. Species I (a_N between 15.1 and 15.8) is molecular solubilized in a lipophilic environment and has considerable mobility despite the use of a solid lipid. It can be attributed to TB molecules molecular dissolved in the lipid alkyl chains. Species II has a very small line width and a large hyperfine splitting of 17.2. It has exactly the same spectral pattern as TB solubilized in water or 2.5% aqueous poloxamer solutions. Therefore, species II can be attributed to TB molecules which are molecular solubilized in the aqueous phase. A competitive nanocompartment for TB in form of tenside micelles can be excluded because poloxamer 188 is known to arrange in micellar structures only at higher concentrations and temperatures (21,22).

A further species (III) has large line widths indicative of spin exchange processes due to a high local concentration. The hyperfine splitting constant (ranges from 16.5 to 16.8) indicates a polar environment. Species III represents TB molecules which are localized in a high local concentration on the surface of the SLN particles. It can be concluded that crystallization of the molten lipid nanodroplets (obtained after high pressure homogenization) leads to an expulsion of the majority of TB molecules (about 70%) onto the particle surface and into the aqueous phase. The ESR spectra of the TB-loaded NLC represent also the three different species. Increasing oil loads lead to decreasing concentrations of species II (TB in the outer aqueous phase). However, increased concentrations of lipid-solubilized TB are only observed at 10% oil load of the lipid phase (NLC-1.0). At lower oil loads (NLC-0.2 and NLC-0.4), TB is preferentially localized in high local concentrations at the particle surface in a more polar environment (species II). Changes in the ESR patterns during storage could not be observed, neither for samples stored at room temperature nor for them at 8°C. Annealing might not play an important role for GB because of its high melting point and its high solidification degree in nanodispersions.

The hydrophilic ascorbic acid reduces accessible TB to an ESR-silent hydroxylamine. The AA assay with aqueous AA solution demonstrates that the examined SLN are not able to protect the lipophilic TB molecule from aqueous reduction medium as it would be expected if liquid lipid domains are surrounded by a solid lipid matrix (Fig. 5). The best protection for the probe is given in a nanoemulsion, which generally is not known as an optimal system of prolonged release. The fastest reduction was observed for SLN, which agrees with the results of the spectral simulation, where the highest amount of TB was attributed to nitroxide molecules localized in polar environments. Generally, diffusion of TB

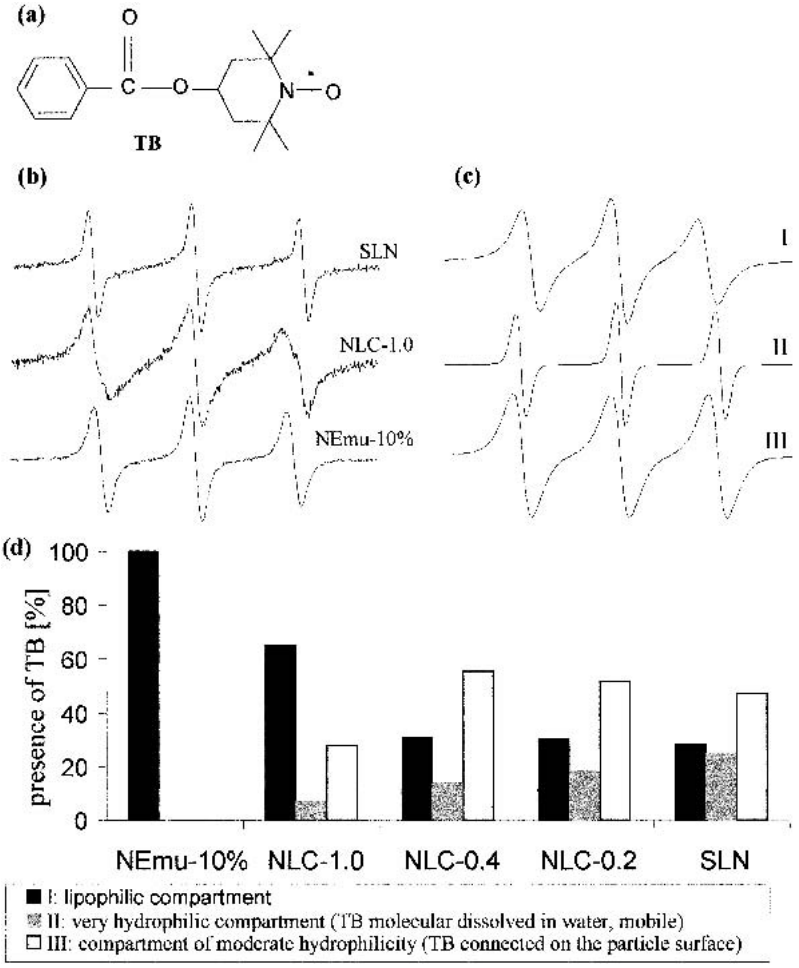

Fig. 4. (a) Chemical structure of tempolbenzoate; (b) GHz ESR spectra of tempolbenzoate (TB) in NEmu-10%, in NLC-1.0, and in SLN (from the bottom to the top); (c) simulated compartments for TB in NLC-1.0, and (d) from simulations calculated localizations of TB in nanodispersions.

inside the particle is rapidly possible due to the very short diffusion length and due to the considerable mobility the TB molecules inside the lipid. Reaching the surface, TB becomes access to the reducing AA (see Fig. 5: the remaining TB concentration in SLN after only 8.5 min is very low). Therefore, the packaging lattice of the small GB platelets must be very loose and incompact.

Changes of the spectral shape were observed during the reduction experiments. The signal intensities of the TB species localized in a polar environment (species II and III) decrease faster than the signal intensity of species I (nonpolar lipid compartment). Interesting conclusions concerning the distribution processes of TB between the polar and the nonpolar microenvironment can be drawn. In a first scenario, no changes in the shape of ESR signals would be seen if distribution happens very fast (e.g., within milliseconds). If the distribution of TB between the different compartments would occur very slowly (e.g., hours), a rapid decrease of the hydrophilic species would be seen and the lipophilic species would remain and dominate the ESR spectrum (scenario two). Our findings correspond to an intermediate scenario where we can clearly detect changes in the spectral shape, but we do not see a dominating signal of the lipophilic species. Therefore, the distribution process of TB between the polar and the nonpolar microenvironment must be comparable to the reduction kinetics of the hydrophilic species and therefore in the order of seconds to minutes.

It is noteworthy that classic release experiments cannot be performed on SLN and NLC because of their colloidal size. Determination of release kinetics for nanodispersions can be done either by Franz flow-through diffusion cells (initially developed for skin permeation studies) or by diluting the formulation in the medium of conventional tablet dissolution testers and later separation of the particles from the medium. Loss of water, choose of membranes/cell layers/media, dilution and separation processes often do not lead to meaningful and comparable data (23) or can even cause artifacts (4,23). So long as these problems exist, ESR spectroscopy at least provides interesting information concerning the accessibility to the drug molecules contained in colloidal carriers, even in a non-invasive way.

Additional experiments were performed where TB was added to the TB-free lipid nanodispersions after the homogenization and tempering steps. The majority of the TB remained as undissolved crystals and diffusion of TB through the water phase is the velocity determining factor in this ex-

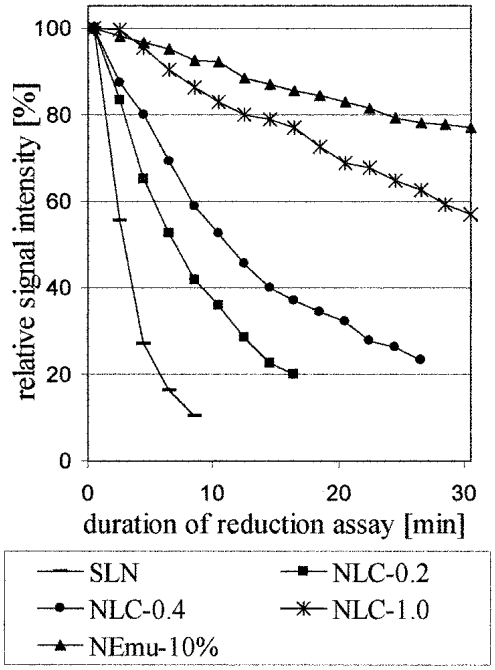

Fig. 5 Decrease of electron spin resonance signal intensity (time against changes in the signal area) of different nanocarrier systems during the ascorbic acid reduction assay.

periment. But after 7 days, some TB molecules were dissolved and distributed in the sample. The recorded ESR spectra were comparable to the regular produced samples at this time point. This indicates that TB can access all compartments if it is added after the production of the nanodispersion.

DSC Measurements

Liquids as water, possible supercooled glyceride fractions, and MCT cannot be registered using the described temperatures and analyzing conditions. Because melting events of GB were detected, supercooled GB particles can be excluded (in agreement with the NMR results of this study; ref. 24). Measurements 1 day and 4 weeks after production led to the same melting pattern. Although the later from a nanoemulsion and from SLN mixed formulations did not differ in their thermal behavior compared to formulation SLN, the MCT loaded samples did (Fig. 6, top panel). First, a depression of the GB melting point can be mentioned, which keeps nearly linear even with oil loads up to 75% (Fig. 6, bottom panel). Second, the difference between the onset point and the peak maxima increased with higher oil load, a signal for more irregular arrangement of molecules (values range from 2.6 K at formulation SLN to 3.9 K at formulation NLC-1.0). These two phenomena show an interaction of oily molecules with the crystalline matrix, but an incorporation can not be claimed necessarily. A depression of the melting point in these fine GB platelets can be provoked even through oil spots or layers on their surface. Just particle shape, colloidal character and particle environment have a big impact on the melting point (25) as particle size distribution (26), too.

It was claimed that MCT localization inside GB particles could be characterized by freezing out the dispersion downwards to temperatures of approximately –60°C (27). Interrelated MCT molecules should result in an endothermic crys-

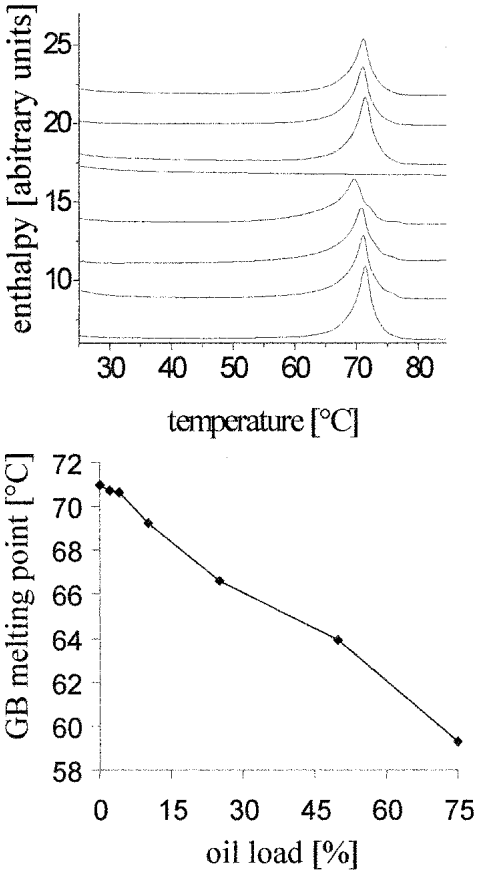

Fig. 6 Top panel: Differential scanning calorimetry heating curves (5 K/min) of formulations SLN, NLC-0.2, NLC-0.4, NLC-1.0, NEmu-10%, Mix-0.2, Mix-0.4, and Mix-1.0 oil load (from the bottom to the top). Graphic below: decrease in glyceryl behenate melting point with increasing medium-chain triclycerides load of nanostructured lipid carriers (experiments done with oil loads from 0 to 75%).

tallization event whereas statistically over the whole GB matrix distributed oil molecules should not be able to form MCT crystals with specific crystallization energy due to the hindering GB barrier. This method was found to be unsuitable for the given measuring problem. Freezing let to crystallize the outer water phase of the dispersion first and unpredictably other components were precipitated in this step. DSC results should be always discussed carefully because the method is invasive and the recorded measuring signals may come from a sample possibly changed by the temperature regime.

X-Ray Measurements

Triglycerides occur in three main modifications α, β', and β which differ in the arrangement of the fatty acids. The arrangement of fatty acid chains can be determined by x-ray measurements. X-ray diffraction patterns of the investigated formulations result in constant reflexes with their maxima at the angles 2 Theta 21.2 and 23.3 (Fig. 7). This correspond to short spacings of the chains at 0.42 and 0.38 nm what is attributed to the β'-modification of the solid lipid (28,29). The presence of diglycerides is known to favor the β'-modification of the lipid (30,31). MCT did not lead to changed patterns, so the lipid crystal structure in x-ray measurements do not seem

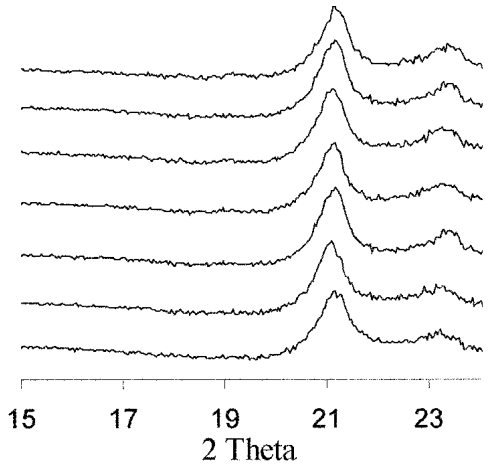

Fig. 7 X-ray diffraction patterns of formulations SLN, NLC-0.2, NLC-0.4, NLC-1.0, Mix-0.2, Mix-0.4, and Mix-1.0 oil load (from the bottom to the top). Formulation NEmu-10% does not provoke reflexes.

to be disturbed by the oil adding. Even after one month of storage the x-ray patterns remain unchanged.

DISCUSSION

SLNs are easy to produce at small and large scale. Our investigated ones are stable over a long period of time with respect to particle size, DSC, x-ray, NMR, and ESR characteristics. For GB particles, annealing could not be observed in the study.

The current experiments on pure and on oil-loaded GB-SLN reveal the common theory of drug localization in the solid lipid particle core as well as the incorporation of oily domains of high drug content in the particles. It should be remembered that all measurements were performed with a lipid consisting of glyceride mixtures with a less ordered matrix in β′-modification. By its numerous defects in crystal lattice GB should facilitate drug incorporation (12,32,33).

The NMR results show an immobilization of the oil in the NLC formulations. The immobilization in MCT–GB particles (formulations NLC-0.2, NLC-0.4, NLC-1.0) is weaker compared to the high immobilization extent of the recrystallized melt of GB bulk containing 2% oil. This is a strong indication that MCT molecules are not well fixed in the solid matrix of the particles. But clear statements if the liquid lipid molecules stay in the inner part of the solid matrix or stick on its outer surface finally cannot be done by NMR. For further information, ESR studies were conducted.

The results of the ESR experiments clearly show that the accommodation of foreign lipophilic molecules is poor for SLN and NLC with low oil load. The majority of TB was pushed out onto the particle surface or into the aqueous phase. Experiments show that TB in SLN systems is rapidly reduced from aqueous AA. The results indicate that the studied colloidal lipid matrices do neither achieve a high incorporation rate nor a protection from the aqueous environment. Instead of the postulated inner oil droplets in the solid matrix, the existence of an emulsion like nanocarrier in this complex system is more probable. Distribution of oil (as molecules or as clusters) inside a crystallized matrix of a nanoparticle is not probable because crystals with their regular structures only

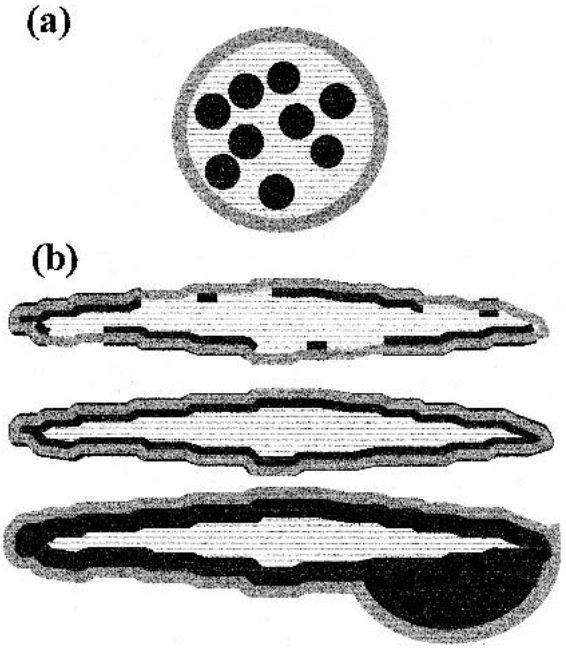

Fig. 8 Schematic structures of nanostructured lipid carriers, (a) model proposed in the literature, (b) models developed because of current experiments, varying with increasing amount of oil loading (oil medium-strain triglycerides), solid lipid (glyceryl behenate), stabilizer (poloxamer)).

tolerate rare defects to incorporate host molecules: The oil is ejected from the molten lipid mix during the lipid crystallization process at the cooling step. Even in case of 2% oil loading (formulation NLC-0.2) oil expulsion happens and therefore the postulated oil incorporation rates up to 16 or 38%, respectively (7,9), cannot be confirmed, not even in an irregular lipid with defects in crystal lattice. In the case that it would have been successfully to incorporate at least this low amount of oil (what could not be found!) it would never be possible to reach a reasonable drug incorporation rate because of low drug solubility capacity in these few MCT molecules. However, if the quantity of liquid lipid in NLC is too small to form droplets, the molecules remain adhered to the solid lipid particle surface (Fig. 8). They form spots or even incomplete films on the particle surface. Additionally, increasing oil rates (from 10% up) lead to the formation of oily droplets sticking on comparatively small GB platelets. In every case, the investigated NLC did not show any advantage with respect to incorporation rate or retarded accessibility to the drug compared to conventional nanoemulsions.

Moreover, the investigated conventional SLN without oil loading by ESR measurements do neither show a protection from aqueous environment (what could be expected due to the solid matrix), nor retardation capacities, nor a sufficient incorporation rate. In all these properties SLN are surpassed by a common nanoemulsion. The drawbacks of SLN are inherent as a result of the crystalline state of the nanocarrier.

ACKNOWLEDGMENT

This work was supported by Deutsche Forschungsgemeinschaft (DFG).

REFERENCES

1. B. Siekmann and K. Westesen. Submicron-sized parenteral carrier systems based on solid lipids. *Pharm. Pharmacol. Lett.* **1**:123–126 (1992).
2. R. H. Müller, W. Mehnert, J.-S. Lucks, C. Schwarz, A. zur Mühlen, H. Weyhers, C. Freitas, and D. Rühl. Solid lipid nanoparticles (SLN)—an alternative colloidal carrier system for controlled drug delivery. *Eur. J. Biopharm.* **41**:62–69 (1995).
3. R. H. Müller, K. Mäder, and S. Gohla. Solid lipid nanoparticles (SLN) for controlled drug delivery—a review of the state of the art. *Eur. J. Biopharm.* **50**:161–177 (2000).
4. W. Mehnert and K. Mäder. Solid lipid nanoparticles: production, characterization and applications. *Adv. Drug Deliv. Rev.* **40**:165–196 (2001).
5. K. Westesen, H. Bunjes, and M. H. J. Koch. Physicochemical characterization of lipid nanoparticles and evaluation of their drug loading capacity and sustained release potential. *J. Control. Release* **48**:223–236 (1997).
6. K. Westesen and B. Siekmann. Investigation of the gel formation of phospholipid-stabilized solid lipid nanoparticles. *Int. J. Pharm.* **151**:35–45 (1997).
7. V. Jenning, A. F. Thünemann, and S. H. Gohla. Characterisation of a novel solid lipid nanoparticle carrier system based on binary mixtures of liquid and solid lipids. *Int. J. Pharm.* **199**:167–177 (2000).
8. R. H. Müller, M. Radtke, and S. A. Wissing. Nanostructured lipid matrices for improved microencapsulation of drugs. *Int. J. Pharm.* **242**:121–128 (2002).
9. V. Jenning, K. Mäder, and S. H. Gohla. Solid lipid nanoparticles (SLN™) based on binary mixtures of liquid and solid lipids: a ^{1}H-NMR study. *Int. J. Pharm.* **25**:15–21 (2000).
10. M. Bockisch. *Nahrungsfette und -öle,* Ulmer, Stuttgart, 1993.
11. A. Fischer-Carius. Untersuchungen an extrudierten und sphäronisierten Matrixpellets mit retardierter Wirkstoffreigabe, Ph.D. Thesis, Free University of Berlin, Berlin, 1998.
12. H. Bunjes, K. Westesen, and M. H. J. Koch. Crystallization tendency and polymorphic transitions in triglyceride nanoparticles. *Int. J. Pharm.* **129**:159–173 (1996).
13. ISO/DIS13320-1. *Korngrößenanalyse–Leitfaden für Laserbeugungsverfahren,* Beuth Verlag, Berlin, Wien and Zürich, 1997.
14. M. Wohlgemuth. Diffusionsexperimente an Nanokapseldispersionen: Größenverteilung, Wirkstoffreisetzung und andere dynamische Phänomene, Ph.D. Thesis, Gerhard-Mercator-Universität, Duisburg, 2002, 194.
15. A. A. Ribeiro and E. A. Dennis. Structure and dynamics by NMR and other methods. In M. J. Schick (ed), *Nonionic Surfactants,* Physical Chemistry, Marcel Dekker, New York, 1987, pp. 971–1009.
16. K. Jores. Characterization of solid lipid nanoparticles (SLN™)—how to optimize the quantity of surfactants. *Proc. Intern. Symp. Control. Release Bioact. Mater.* **27**:1092–1093 (2000).
17. H. Bunjes, M. Drechsler, M. H. J. Koch, and K. Westesen. Incorporation of the model drug ubidecarone into solid lipid particles. *Pharm. Res.* **18**:287–293 (2001).
18. H. Bunjes, B. Siekmann, and K. Westesen. Emulsions of supercooled melts—a novel drug delivery system. In S. Benita (ed), *Submicron Emulsions in Drug Targeting and Delivery,* Harwood Academic Publishers, Chur, 1998, pp. 175–204.
19. C. Mayer, D. Hoffmann, and M. Wohlgemuth. Structural analysis of nanocapsules by nuclear magnetic resonance. *Int. J. Pharm.* **242**:37–46 (2002).
20. K. Mäder, H. M. Swartz, R. Stösser, and H.-H Borchert. The application of EPR spectroscopy in the field of pharmacy. *Pharm. Unserer Zeit* **49**:97–101 (1994).
21. BASF. Technical information for Lutrol F 68™. (1997).
22. P. Alexandridis and T. A. Hatton. Poly(ethylene oxide)-poly(propylene oxide)-poly(ethylene oxide) block copolymer surfactants in aqueous solutions and at interfaces: thermodynamics, structure, dynamics, and modeling. *Coll. Surf. B* **96**:1–46 (1995).
23. A. Haberland, C. S. Maia, K. Jores, M. Dürrfeld, W. Mehnert, I. Schimke, B. Christ, and M. Schäfer-Korting. Albumin effects on drug absorption and metabolism in reconstructed epidermis and excised pig skin. *Altex* **20**:3–9 (2003).
24. K. Westesen and H. Bunjes. Do nanoparticles prepared from lipids solid at room temperature always possess a solid lipid matrix? *Int. J. Pharm.* **115**:129–131 (1995).
25. B. Siekmann and K. Westesen. Thermoanalysis of the recrystallization process of melt-homogenized glyceride nanoparticles. *Coll. Surf. B* **3**:159–175 (1994).
26. H. Bunjes, M. H. J. Koch, and K. Westesen. Effect of particle size on colloidal solid triglycerides. *Langmuir* **16**:5234–5241 (2000).
27. V. Jenning. Feste Lipid-Nanopartikel (SLN™) als Trägersystem für die dermale Applikation von Retinol: Wirkstoffinkorporation, -freisetzung und Struktur, Ph.D. thesis, Freie Universität Berlin, 1999.
28. K. Larsson. Classification of glyceride crystal forms. *Act. Chem. Scand.* **20**:2255–2260 (1966).
29. D. M. Small. *The Physical Chemistry of Lipids: from Alkanes to Phospholipids,* Plenum Press, New York, 1986.
30. J. W. Hagemann. Thermal behavior and polymorphism of acylglycerides. In K. Sato and N. Garti (eds), *Crystallization and Polymorphism of Fats and Fatty Acids,* Marcel Dekker, New York and Basel, 1988, pp. 9–95.
31. L. Hernqvist. Crystal structures of fats and fatty acids. In K. Sato and N. Garti (eds), *Crystallization and Polymorphism of Fats and Fatty Acids,* Marcel Dekker, New York and Basel, 1988, pp. 97–137.
32. D. Precht. Fat crystal structure in cream and butter. In N. Garti and K. Sato (eds), *Crystallization and Polymorphisms of Fats and Fatty Acids,* Marcel Dekker, New York and Basel, 1988, pp. 305–361.
33. V. Jenning and S. Gohla. Comparison of wax and glyceride solid lipid nanoparticles (SLN™). *Int. J. Pharm.* **196**:219–222 (2000).